Magnetic domain structures in ultrathin $Fe_xNi_{(1-x)}$ films on Cu(111): Dependence on film thickness and stoichiometry

Y. Sato, T. F. Johnson, S. Chiang,[a] J. A. Giacomo, and X. D. Zhu
Department of Physics, University of California, Davis, California 95616

D. P. Land
Department of Chemistry, University of California, Davis, California 95616

F. Nolting[b] and A. Scholl
Advanced Light Source, Lawrence Berkeley National Laboratory, Berkeley, California 94720

(Received 20 September 2002; accepted 6 October 2003; published 8 January 2004)

The magnetic domain structures in thin $Fe_xNi_{(1-x)}$ alloy films grown on Cu(111) have been investigated by the photoemission electron microscope (PEEM). By tuning the photon energy to respective x-ray absorption edges, element-specific information can be obtained with PEEM. We have observed clear ferromagnetic domains on samples with an iron concentration of $x \leqslant 0.6$ and $x = 1.0$. The PEEM images indicate that Fe and Ni form a good alloy on Cu(111), with the same domain structures and the magnetization in each domain aligned for both elements. The domain sizes and shapes exhibit dependence on thickness, stoichiometry x, and substrate quality. © *2004 American Vacuum Society.* [DOI: 10.1116/1.1631295]

I. INTRODUCTION

Controlling the synthesis and characterizing the resultant properties of ultrathin metal films at the atomic monolayer level is critical for a better understanding of magnetotransport properties of such films and their technological use in the magnetic storage industry. For example, interdiffusion is known to have detrimental effects on the giant magnetoresistive effect in Cu/FeNi/Cu systems which are relevant to spin valve magnetic disk drive heads. When the intermixed region is reduced to 1 Å or less, the effect is expected to increase considerably.[1] We have studied thin $Fe_xNi_{(1-x)}$ alloy films grown on Cu(111) for their relevance to the above mentioned technology.

FeNi alloys have also been a subject of intense study because of the Invar effect manifested in $Fe_{65}Ni_{35}$ alloys.[2–7] The bulk alloys show anomalous behavior when the Fe concentration approaches ~65%. When the structural transformation from the face-centered-cubic (fcc) to the body-centered-cubic (bcc) phase occurs, the Curie temperature and the magnetic moment collapse, simultaneously. It has long been known that the effect is related to magnetism[8] but its origin is still not well understood.[9] Gaining control over the synthesis of these films and characterizing the system in a comprehensive manner will allow us to better address this question of interest.

In recent years, molecular-beam epitaxy has been used for layer-by-layer synthesis of epitaxial $Fe_xNi_{(1-x)}$ films on Cu substrates.[3–6,10] Techniques, such as low-energy electron diffraction (LEED),[5,6] reflection high-energy electron diffraction (RHEED),[5,6] photoelectron diffraction,[4] surface magneto-optical Kerr effect (SMOKE),[5,6] x-ray photoemission spectroscopy with the technique of x-ray magnetic linear dichroism (XMLD),[6,12] Mossbauer spectroscopy,[2,3] and superconducting quantum interference device (SQUID) magnetometry,[3] have been applied to characterize the dependence of the crystal structure, the macroscopic magnetization, and the local magnetic moments on the composition in the alloys. One important factor in characterizing a magnetic system is information on the domain structures. The above mentioned techniques, however, lack the ability to spatially determine the microscopic magnetic structure of the thin films. Though the ferromagnetic (FM) domain structure in bulk $Fe_xNi_{(1-x)}$ alloys has been studied for Permalloy and Perminvar by neutron scattering and complex permeability measurement,[11] no such study has been performed on thin films. Here, we report photoemission electron microscope (PEEM) images of the FM domain structure in ultrathin films of $Fe_xNi_{(1-x)}$, grown epitaxially on Cu(111). We have used the PEEM to directly observe the domain structure of the films and its dependence on thickness, stoichiometry x, and substrate quality.

II. EXPERIMENT

The experiments were performed with the PEEM2 facility on beamline 7.3.1.1 at the Advanced Light Source at Lawrence Berkeley National Laboratory. The focused circularly polarized x rays were incident on the sample at an angle of 30° from the surface. The PEEM2 microscope images low-energy secondary photoelectrons from the sample with magnification onto a phosphor screen that is read by a charge-coupled device camera. The spatial resolution of PEEM2 is limited to 20 nm by chromatic aberrations.[12]

Samples were prepared in the preparation chamber attached to the PEEM chamber (base pressure $\sim 7 \times 10^{-10}$ Torr in the preparation chamber and 1×10^{-9} in the PEEM chamber). The Cu(111) crystal was mechanically polished and, for some samples, subsequently electropolished

[a]Electronic mail: chiang@physics.ucdavis.edu
[b]Present address: Swiss Light Source, Paul Scherrer Institut, CH 5232 Villigen PSI, Switzerland.

before inserting it into the vacuum system. The surface was cleaned by cycles of Ar-ion bombardment (1.5 kV, 2×10^{-7} Torr) and annealing. The alloy films of two different thicknesses [5 monolayers (ML) and 10 ML] were grown at room temperature by coevaporation of Fe and Ni onto the Cu(111) substrate. The growth rates of the Fe and Ni sources were calibrated separately immediately before the preparation of each sample. The typical growth rate for a film was 0.8 ML/min. We have systematically changed the concentration of the $Fe_xNi_{(1-x)}$ alloy films. We studied a total of 16 samples ($x=0$, 0.28, 0.55, 0.6, 0.66, 0.74, and 1.0 at ~10 Å≈5 ML, and $x=0.9$, 0.25, 0.33, 0.42, 0.44, 0.5, 0.55, and 1.0 at ~20 Å≈10 ML). LEED patterns observed for several samples showed six-fold symmetry in agreement with the fcc lattice structure.

The imaging of magnetic domains with the PEEM makes use of the x-ray magnetic circular dichroism (XMCD) effect that arises at the x-ray absorption edges. Domains on the sample that have different geometric projections of the magnetization direction onto the direction of the incoming *x* rays show a different absorption cross section for circularly polarized light.[13,14] In the case of $Fe_xNi_{(1-x)}$ films, the domain pattern for Fe (Ni) is enhanced by taking the difference of the two images acquired at the Fe (Ni) $L3$ and Fe (Ni) $L2$ edges. Since the XMCD signal changes its sign when switching from the $L3$ to the $L2$ edge, stronger contrast arises. Element selectivity is ensured by tuning the photon energy to the characteristic absorption edges, and the surface sensitivity is attributed to the limited escape depth of the electrons (~2–10 nm) used to form the PEEM image.[15–17]

III. RESULTS

Samples with high Fe content ($x=0.66$ and 0.74 at 5 ML) were observed to be nonmagnetic at 300 K. All other alloy samples ($x\leqslant0.6$, 5 and 10 ML) showed clear ferromagnetic contrast. This trend of reduction in the Curie temperature at a higher Fe concentration had also been observed by XMLD.[18] We also found that a pure Ni film at 5 ML thickness was nonmagnetic at 300 K. According to a SMOKE measurement, 5 MLs is approximately the thickness where the Curie temperature becomes less than 300 K for Ni/Cu(111).[19]

Figures 1(a) and 1(b) show FM contrast images for Fe and Ni, measured on a 10 ML thick $Fe_{0.42}Ni_{0.58}$ alloy film. The contrast visible in these images is clearly FM since the contrast in the image acquired at the $L3$ absorption edge reverses in the image at $L2$ edge. The two images unambiguously show that Fe and Ni have the same domain structures with their magnetization aligned. This observation is consistent for every sample analyzed. We can, therefore, conclude that these two elements form a good alloy on the Cu(111) surface. The strength of the contrast is in proportion to the dichroism effect at the two absorption edges used for imaging. As illustrated in the two images of Figs. 1(a) and 1(b), the Ni dichroism is always smaller than the Fe dichroism. Thus, all other magnetic images shown in this article are Fe magnetic contrast images for clearer contrast.

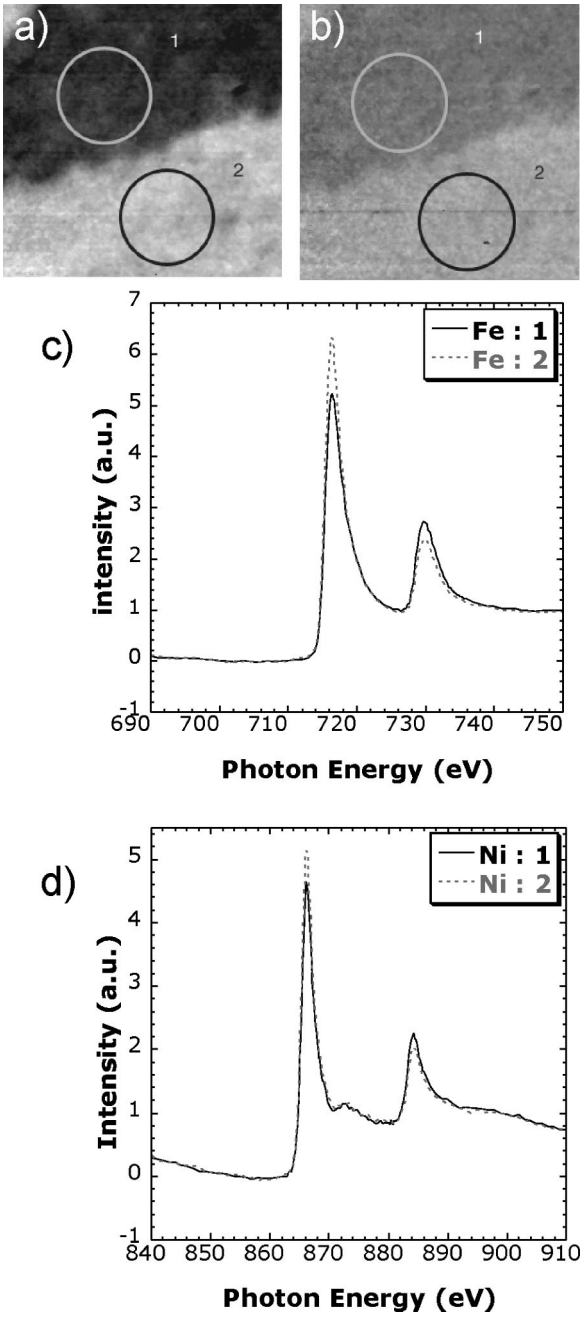

FIG. 1. (a) Fe and (b) Ni contrast in XMCD FM images with a 6 μm×6 μm field of view for a 10 ML sample, $x=0.42$. (c) Fe and (d) Ni magnetic circular dichroism spectra of $L3$ and $L2$ edges from two different regions (labeled 1 and 2) in (a) and (b).

Figures 1(c) and 1(d) show the local x-ray absorption spectra obtained for Fe and Ni in regions 1 and 2 of Figs. 1(a) and 1(b). The spectra clearly show magnetic dichroism at the two absorption edges. This analysis confirms that the contrast in the images arises from the difference of the magnetization directions in these regions and is not of a topographic nature.

Next, we would like to discuss the dependence of the domain structures of the alloy films on the film thickness and substrate quality. Figure 2 shows typical images from the 5 ML samples with varying concentration. No consistent pat-

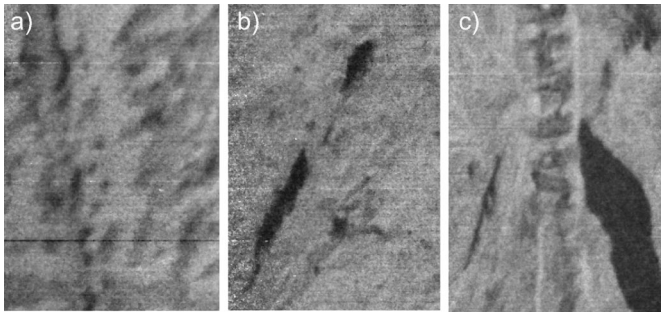

FIG. 2. Fe XMCD FM images with a H 22 μm$\times V$ 30 μm field of view for 5 ML samples with varying Fe concentration x: (a) $x=0.28$, (b) $x=0.55$, and (c) $x=0.6$.

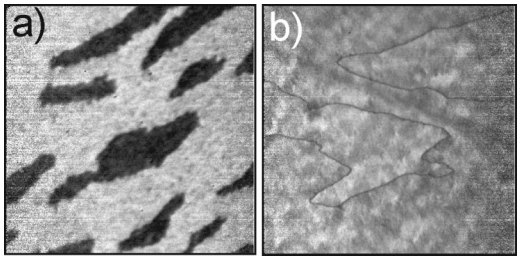

FIG. 4. Fe XMCD images for 10 ML samples showing domain structures which are typical for Fe concentration of $x=0.42$ to 0.55. The arrows indicate the magnetization direction within each domain: (a) $x=0.42$ and (b) $x=0.44$, with crystal substrate rotated approximately 90° with respect to the substrate in the previous image.

tern was observed at this thickness; instead, the magnetic structures appear to reflect topographic features of the surface. Similar features were observed in the images acquired at the preabsorption edge for magnetic samples and those acquired at absorption edges for nonmagnetic samples at 300 K. In those images, the contrast arises from topographic structures and the difference in the work function of the surface. This observation supports the view that, for 5 ML thickness on a mechanically polished substrate, the formation of domain structures is strongly influenced by the surface topographic features. When $Fe_{0.28}Ni_{0.72}$ and $Fe_{0.55}Ni_{0.45}$ (5 ML) samples were annealed above the Curie temperature, the magnetic contrast which had been observed at 300 K gradually disappeared. Magnetic contrast was recovered again as the sample temperature was lowered below the Curie temperature, confirming that the observed domain structures were pinned by geometric features on the surface.

In contrast, 10 ML samples on an electropolished substrate showed very different domain structures for three different concentrations (Fig. 3). First, pinning of domains due to surface defects was observed much less frequently. Another striking difference is the concentration dependence of the domain structures, which is clearly depicted in the three images shown in Fig. 3. At the lower Fe content of $x=0.33$, the domains are much smaller in size, and large portions of the surface have ambiguous contrast of gray with varying shades. The average diameter of the circular island-like domains was ~ 0.8 μm, which is an order of magnitude smaller than the typical domain size observed on samples with higher Fe content. At the increased Fe concentrations of $x=0.42$ and $x=0.55$, the dominant domain structures are of an elongated shape, and the contrast between domains of different magnetization is very clear. The size of these elongated structures varies from smaller domains, ~ 2.5 μm length and ~ 1 μm width, to larger ones, ~ 20 μm length and ~ 4 μm width. The two clearly defined shades in the images indicate that there is a preferred direction of magnetization, and the magnetization in each domain is aligned along that direction. In this case, domains that appear dark have their magnetization mostly antiparallel to the projection of the photon angular momentum, and vice versa for the regions that have lighter shades. The images of $Fe_{0.33}Ni_{0.67}$ films, for thicknesses of both 5 and 10 ML, indicate that there is no such preferred direction for magnetization in those samples. Figure 3(d) shows a magnetic contrast image of a 10 ML $Fe_{0.5}Ni_{0.5}$ film. This sample, in contrast to other 10 ML samples at a concentration range of 42%–55%, showed little domain structure. The structures of the films were similar to 10 ML films of lower Fe concentration. More experiments are necessary to explain the different domain structures of samples with a similar concentration.

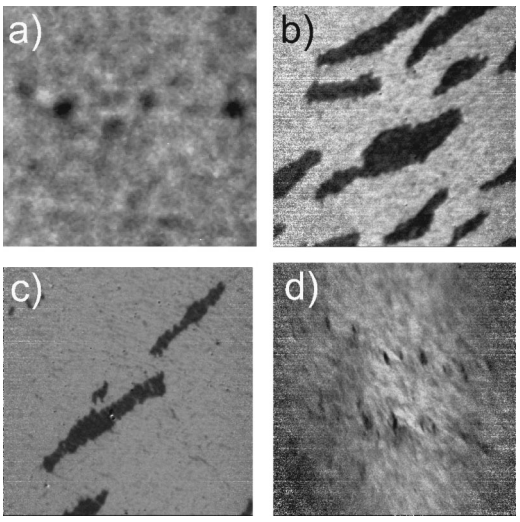

FIG. 3. Fe XMCD ferromagnetic images for 10 ML samples with varying Fe concentration x: (a) $x=0.33$, 10 μm$\times$10 μm, (b) $x=0.42$, 40 μm$\times$40 μm, (c) $x=0.55$, 40 μm$\times$40 μm, and (d) image of another film showing little domain structure, $x=0.5$, 65 μm$\times$65 μm.

Figure 4 shows two different 10 ML films for Fe concentrations of $x=0.42$ and $x=0.44$, each showing the typical domain structures observed at these Fe concentrations. The difference in contrast in both images arises from the difference in the relative orientation of the magnetization and the projection of the angular momentum of the incident photon. Very high contrast between domains is observed in Fig. 4(a), suggesting that the magnetization vectors are in the plane and are nearly parallel or nearly antiparallel to the projection of the angular momentum of the incident photon. If this is the case, rotating the sample by 90° would result in the nearly complete loss of contrast between magnetic domains, except for domain walls. Indeed, this loss of contrast is seen

in Fig. 4(b), for which the photon angular momentum remained the same, while the crystal substrate was rotated approximately 90°. The domain walls are clearly visible as dark lines in Fig. 4(b), as a result of the continuous rotation of the magnetization by 180° within the domain walls. The width of the domain walls is on the order of 1 μm.

IV. DISCUSSION

Previous studies on $Fe_xNi_{(1-x)}$ alloy films grown on Cu(100) showed two important results concerning the structure and growth of the films.[5,6,10] First, the alloy films grow epitaxially in the fcc phase for the entire concentration range of Fe. At higher coverage ($\sim$4 ML), however, a small reduction of the in-plane lattice constant (0.7%–1% compared to the substrate parameter) is observed for samples of a higher Fe concentration.[5] Nevertheless, no abrupt structural change into the bcc phase is indicated, unlike the bulk form. Second, RHEED experiments indicate good layer-by-layer growth, independent of thickness and concentration. Small deviations in the crystal structure were observed for films of a higher Fe concentration ($x=0.77$ and 0.8),[5] but the fcc phase appears to prevail. On Cu(111), similar epitaxial growth was observed by RHEED experiments, and additional x-ray diffraction measurements confirmed that no bcc phase was present in the films over the entire Fe concentration range.[3]

Studies using SMOKE, XMLD, and SQUID have found that the alloy films on Cu(100) and Cu(111) show ferromagnetic signals for all Fe concentrations.[3–6,18] We have confirmed the ferromagnetic state of films on Cu(111) up to $x=0.6$ which show clear FM domains at room temperature. On Cu(100), a drop in magnetization and anomalous behavior of T_C was observed for $\sim$65% Fe content. We have observed both of these phenomena on the Cu(111) surface, as discussed above. For the case of $Fe_xNi_{(1-x)}/Cu(100)$, it has been suggested that a magnetic phase transition from a high spin FM state into another phase takes place at the above mentioned concentration, which is also manifested by the change in lattice parameters. In fact, a close connection between the Fe magnetization and the atomic volume has been found.[6] On Cu(111), no detailed study on the structural evolution of the films is available to determine the correlation between the observed magnetic change and the atomic volume. The comparable growth of the alloy films and similar magnetic behavior observed on two different surfaces, however, imply that the magnetic behavior of the alloy films on Cu(111) may also be explained by the change in the atomic volume. If that is true, the increase in film magnetization from a lower x content to $x\sim0.5-0.6$, which is observed by SQUID[3] and XMLD,[18] suggests that the increase in the atomic volume for Cu(111) is similar to that for Cu(100).

How is the domain structure of the film affected by this change in magnetism? Our magnetic contrast images show that, at 10 ML thickness on an electropolished substrate, typical domain sizes increase from a lower Fe content to $x=0.6$. For 5 ML films on a mechanically polished substrate, domain structures appear to be strongly correlated with the topographic features of the surface. On 10 ML films, we have also observed characteristic elongated domains on samples with a higher Fe content ($0.42\leqslant x\leqslant 0.6$). Above $x=0.66$, films were observed to be nonmagnetic at room temperature, indicating a magnetic transition in process accompanied by a drop in T_C. It is interesting to note that the Ni magnetization appears to be independent of Fe concentration.[18,20] This may be due to the fact that the Ni lattice parameter ($a=3.52$ Å) is much closer to that of the Cu substrate ($a=3.61$ Å) than that of Fe ($a=2.87$ Å), so that the strain due to the epitaxial growth does not affect the Ni magnetic moment as much.

V. CONCLUSION

Despite this observed difference in the magnetism of Fe and Ni, the two elements have the same domain structures, with their magnetization aligned as shown. From this observation, we conclude that the two elements form a good alloy with no evidence of segregation on the Cu(111) surface. Domain structures were pinned by topography for 5 ML samples of varying concentration on mechanically polished substrates. For electropolished substrates, sharp magnetic domain constrast was not correlated with topography. For a Fe concentration of $x\geqslant 0.6$, the films were nonferromagnetic at room temperature, agreeing with previous results showing reduced Curie temperature.[18] For the bulk alloy, $x\geqslant 0.65$ is approximately the concentration where the Curie temperature and the magnetic moment collapse as mentioned before. For a 10 ML film with $x=0.42$, 0.44, and 0.55, the magnetization was in plane, and rotation of the sample with respect to the photon polarization showed 180° domain walls.

ACKNOWLEDGMENTS

This work was partially supported by the Campus Laboratory Collaboration Program of the University of California Office of the President. The Advanced Light Source is supported by the Director, Office of Science, Office of Basic Energy Sciences, Materials Sciences Division, of the U.S. Department of Energy under Contract No. DEAC03-76SF00098 at Lawrence Berkeley National Laboratory.

[1] T. C. Huang, J.-P. Nozieres, V. S. Speriosu, H. Lefakis, and B. A. Gurney, Appl. Phys. Lett. **60**, 1573 (1992).
[2] S. H. Mahmood, K. K. Rousan, A.-F. Lehloof, and S. S. Mahmoud, Solid State Commun. **95**, 879 (1995).
[3] J. W. Freeland, I. L. Grigorov, and J. C. Walker, Phys. Rev. B **57**, 80 (1998).
[4] R. Schellenberg, H. Meinert, N. Takahashi, F. U. Hillebrecht, and E. Kisker, J. Appl. Phys. **85**, 6214 (1999).
[5] F. O. Schumann, S. Z. Wu, G. J. Mankey, and R. F. Willis, Phys. Rev. B **56**, 2668 (1997).
[6] F. O. Schumann, R. F. Willis, K. G. Goodman, and J. G. Tobin, Phys. Rev. Lett. **79**, 5166 (1997).
[7] F. O. Schumann, M. Hochstrasser, R. F. Willis, K. G. Goodman, and J. G. Tobin, J. Magn. Magn. Mater. **198**, 522 (1999).
[8] Y. Ishikawa, S. Onodera, and K. Tajima, J. Magn. Magn. Mater. **10**, 183 (1979).
[9] M. van Schilfgaarde, I. A. Abricosov, and B. Johansson, Nature (London) **400**, 46 (1999).
[10] M. G. Martin, E. Foy, F. Chevrier, G. Krill, and M. C. Asensio, Surf. Sci. **433**, 88 (1999).

[11]G. Ban, L. Koszegi, and S. S. Shilstein, J. Magn. Magn. Mater. **83**, 384 (1990); Permalloy (76.4% Ni, 5.2 wt % Cu, 4.0 wt % Mo, 0.7 wt % Mn, R:Fe) and Perminvar (36.0 wt % Ni, 0.3 wt % Mn, R:Fe).
[12]S. Anders, H. A. Padmore, R. M. Duarte, T. Renner, M. R. Scheinfein, J. Stohr, L. Seve, and B. Sinkovic, Rev. Sci. Instrum. **70**, 3973 (1999).
[13]J. Stohr, Y. Wu, B. D. Hermsmeir, M. G. Samant, G. R. Harp, S. Koranda, and D. Dunham, Science **259**, 658 (1993).
[14]J. Stohr, H. A. Padmore, S. Anders, T. Stammler, and M. R. Scheinfein, Surf. Rev. Lett. **5**, 1297 (1998).
[15]R. Nakajima, J. Stohr, and I. Idzerda, Phys. Rev. B **59**, 6421 (1999).
[16]R. G. Jones and D. P. Woodruff, Surf. Sci. **114**, 38 (1982).
[17]J. Stohr and S. Anders, IBM J. Res. Dev. **44**, 535 (2000).
[18]T. F. Johnson, S. Chiang, Y. Sato, D. A. Arena, S. A. Morton, M. Hochstrasser, J. G. Tobin, J. D. Shine, J. A. Giacomo, G. E. Thayer, D. P. Land, and X. D. Zhu, Mater. Res. Soc. Symp. Proc. **674**, U7.9 (2001).
[19]R. Zhang and R. F. Willis, Phys. Rev. Lett. **86**, 2665 (2001).
[20]J. G. Tobin and F. O. Schumann, Surf. Sci. **478**, 211 (2001).